Int j simul model 7 (2008) 2, 93-105
ISSN 1726-4529 Original scientific paper

SIMULATION OF CUTTING FORCES FOR COMPLEX SURFACES IN BALL-END MILLING

Smaoui, M.; Bouaziz, Z. & Zghal, A.
Unit of Mechanics, Solids, Structures and Technological Development,
Ecole supérieure des sciences et techniques, BP 56 Beb Mnara, 1008 Tunis, TUNISIA
E-Mail : smaouimoez@voila.fr; zoubeir.bouaziz@enis.rnu.tn; ali.zghal@esstt.rnu.tn

Abstract
This article presents a method of a cutting force prediction in the case of a ball-end milling. We have proposed a geometrical description of a generic tool so as to simulate the 3 axis milling operation with a hemispherical ball-end cutter. This tool is decomposed into elementary discs; a mechanical approach of the cut is applied onto each disc to obtain the cutting forces from the machined material behaviour and from the cutting conditions. The model, thus obtained, will be afterward generalised in the case of an inclined or circular surface. This generalisation is carried out by adopting, at each time, an adequate reference change, dependent on the trajectory inclination angle. For application, we will consider the milling of a complex part. In fact, the synthesized cut model will be applied to the different types of surfaces which constitute this workpiece; and this will be executed according to the two machining senses: longitudinal and transversal.
(Received in January 2008, accepted in May 2008. This paper was with the authors 1 month for 1 revision.)

Key Words: Ball-End Milling, Cutting Force, Complex Surface

1. INTRODUCTION

The ball end milling is the most frequent in the machining of mechanical work pieces with complex surfaces [1, 2]. The machining of these work pieces presents several difficulties such as the complex geometry of certain parts, very hard materials or the great precision… This latter is a determining factor which has an influence upon the milling operation performances. Another factor, which is not less important, is the tool life.

In order to improve the ball-end milling performance, several researches got interested in the study and in the modeling of the cutting forces.

Fontaine & al. [3-5] present a thermo-mechanical model which takes into account the friction on the rake face and on the relief face, so as to obtain a thermic modeling of the cutting zone. Yang [6] and Lee & Altintas [7] estimate the cutting forces from the machining parameters, from the workpiece, from the tool material, and from the geometry of this latter [2, 6, 7].

The prevision of these forces allows, then, to optimize the process [8] and consequently to improve the reliability, the precision and the productivity.

In this work, we will be focused on the cutting forces modeling. In this way, the first part is devoted to the geometrical study of the cutting tool, so that we could determine, in a second part, the corresponding cutting forces.

Afterwards, we are going to transform the cutting forces model, in order to generalize it to the complex surfaces case. In fact, we will present the model in the case of an inclined and circular surface. These models will be applied in the case of a complex part milling. To be able to carry out the milling of this work piece, we will present the simulated force for the different types of surfaces, which make up the workpiece, such as the inclined upward/downward surfaces and the convex/concave surfaces…

Besides, the milling will be achieved according to the two senses: lengthwise and width-wise. This work will end with a conclusion and some perspectives.

2. CUTTING TOOL MODEL

The geometry of a ball-end cutter can be decomposed into two parts: a cylindrical part with a constant helix angle i_0, and a spherical part of a same radius R, the modeling of which will be given in details further on.

In order to modelize the cutting forces, it is essential to know the geometry of the spherical part. This latter will be discretized into a series of elementary discs. Let's take the case of a point P of a disc, whose radius $R(z)$ belongs to the z coordinate of the cutting edge in a cartesian coordinate system $\Re_C\,(O, X, Y, Z)$, as shown in the following figure.

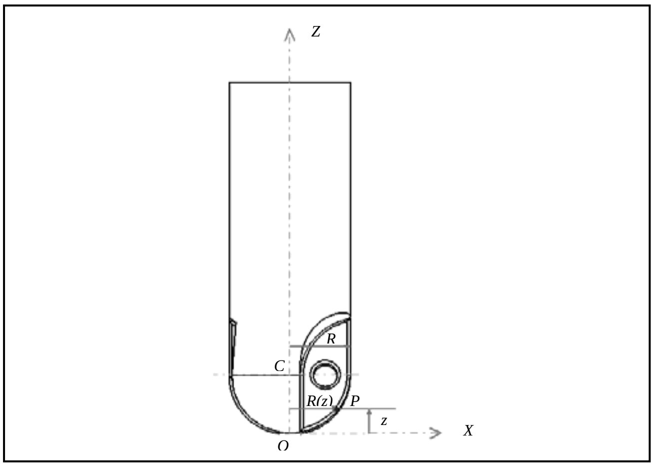

Figure 1: Example of a ball-end tool.

The local radius $R(z)$ of the elementary disc or of each circumference can be given in the following form:

$$R(z) = \sqrt{R^2 - (R - z)^2} \tag{1}$$

The radius $R(z)$ is the local radius of the elementary disc in the plan X-Y which respects the following relation:

$$\eta = \arcsin \frac{R(z)}{R} \tag{2}$$

where η is the angular position following the Z-axis, starting from the C centre of the hemi-sphericalpart towards the infinitesimal cutting edge.

For the same value of z, there is an element decomposed for each tooth. In order to define the position of each of them, we define the angle φ_p which is the angle between the two consecutive teeth:

$$\phi_p = \frac{2\pi}{N_f} \tag{3}$$

with N_f the number of teeth. If we decompose the angle φ_p into N_θ increments, each of these increments is represented by the index j (j = 1, 2, …, N_θ). So, the angular position of the considered cutting edge is given by:

$$\theta(\,j\,) = j\left(\frac{\phi_p}{N_\theta}\right),\ j = 1, 2, \ldots, N_\theta \tag{4}$$

The cutting edges, engaged in the material at an axial depth of cut A_d, are decomposed into N_z elementary cutting edges, which are supposed to be linear, according to an axial discretization increment dz, where each of which bears the index i ($i = 1, 2, \ldots, N_z$), see Fig. 2.

$$dz = \frac{A_d}{N_z} \tag{5}$$

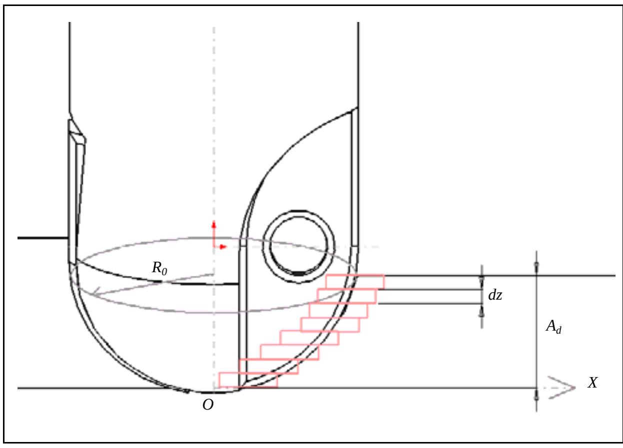

Figure 2: The cutting edge discretization.

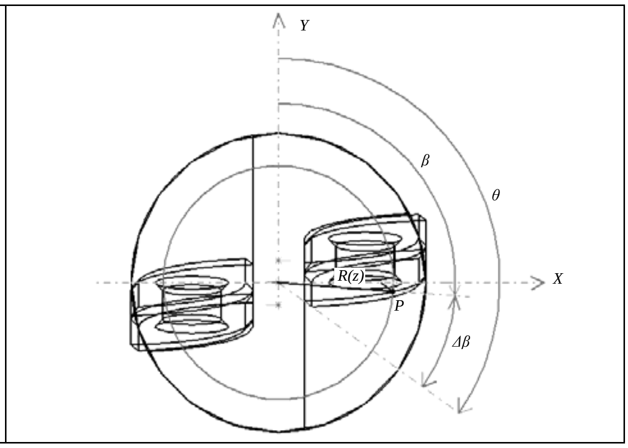

Figure 3: Angular position of the cutting edge in the plan X-Y.

The point P, on the cutting edge k, is found to be in an axial position i, and in a $\beta(i, j, k)$ angular position around the axis, measured from the axis Y (Fig. 3). It is defined by:

$$\beta(i,j,k) = \theta(j) + \phi_p(k-1) - \frac{z}{R(z)} \tan i_0 \tag{6}$$

In the Cartesian coordinate system $\Re_C(O, X, Y, Z)$, the coordinate z of the elementary disc centre, following the direction of the tool Z-axis, is:

$$z = (i-1)dz + \frac{dz}{2} \tag{7}$$

The chip thickness denoted h_b is obtained by the equation of Martelotti, modified [9], taking into account the angular radial and axial position, shown in Fig. 4:

$$h_b = f_{z_b} \sin\beta \sin\eta \tag{8}$$

where f_{z_b} is the feeding per tooth.

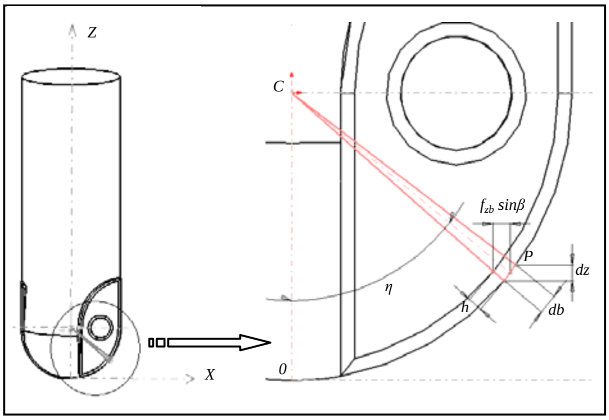

Figure 4: The uncut chip thickness.

The general equation of the uncut chip thickness is then:

$$h_b(i,j,k) = f_{z_b} \sin[\beta(i,j,k)] \sin[\eta(i)] \tag{9}$$

3. CUTTING FORCES MODEL

For an elementary cutting edge, we introduce a spherical coordinate system $\Re_S$, having as origin the spherical part centre C and the unitary local vectors ($\vec{R}, \vec{T}, \vec{A}$) which follow respectively the radial direction, the decreasing β direction and the increasing η direction.

Three components with an infinitesimal force are locally defined at a point P of the cutting edge K ($K = 1 \ldots N_f$). These three components F_R, F_T and F_A are defined in the local coordinate system $\Re_S$, according to the following figure.

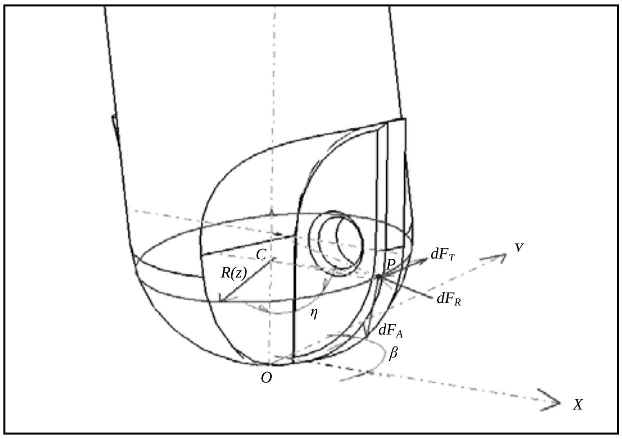

Figure 5: Cutting forces applied to the tool.

The equations of the elementary radial, tangential and axial cutting forces [10], represented in Fig. 5, are:

$$\begin{cases} dF_R = K_R\ h_b\ db = K_R\ f_{z_b}\ sin\,\beta\ sin\,\eta\ db \\ dF_T = K_T\ h_b\ db = K_T\ f_{z_b}\ sin\,\beta\ sin\,\eta\ db \\ dF_A = K_A\ h_b\ db = K_A\ f_{z_b}\ sin\,\beta\ sin\,\eta\ db \end{cases} \tag{10}$$

where K_R is the specific radial coefficient, K_T is the specific tangential coefficient and K_A the specific axial coefficient.

In order to determine the chip surface on an infinitesimal cutting edge and in the case of a ball-end milling cutter, the height of the cutting edge discretized part has been considered similar to the axial thickness of the elementary disc dz. The thickness db can be determined according to the position of this cutting edge.

$$db = \frac{dz}{sin\,\eta} \tag{11}$$

By inserting the equation (11) into (10), then we obtain:

$$\begin{cases} dF_R = K_R\ f_{z_b}\ sin\,\beta\ dz \\ dF_T = K_T\ f_{z_b}\ sin\,\beta\ dz \\ dF_A = K_A\ f_{z_b}\ sin\,\beta\ dz \end{cases} \tag{12}$$

The equation generalized for the elementary radial, tangential and axial cutting forces is given by:

$$\begin{cases} dF_R(i,j,k) = K_R\ f_{z_b}\ sin[\beta(i,j,k)]\,dz \\ dF_T(i,j,k) = K_T\ f_{z_b}\ sin[\beta(i,j,k)]\,dz \\ dF_A(i,j,k) = K_A\ f_{z_b}\ sin[\beta(i,j,k)]\,dz \end{cases} \tag{13}$$

These cutting forces can also be calculated according to the elementary forces expressed in the Cartesian coordinate system $\Re_C$ such as:

$$\begin{cases} dF_R = -\sin\eta\,\sin\beta\;dF_X - \sin\eta\,\cos\beta\;dF_Y + \cos\eta\;dF_Z \\ dF_T = -\cos\beta\;dF_X + \sin\beta\;dF_Y \\ dF_A = -\cos\eta\,\sin\beta\;dF_X - \cos\eta\,\cos\beta\;dF_Y - \sin\eta\;dF_Z \end{cases} \tag{14}$$

We put $[T]_{\Re_C}^{\Re_S}$ the matrix of the passage from $\Re_S\ (C, \vec{R}, \vec{T}, \vec{A})$ towards $\Re_C\ (O, X, Y, Z)$. The cutting forces defined in the Cartesian coordinate system $\Re_C$ are, therefore, expressed by:

$$\{dF_{X,Y,Z}\} = [T]_{\Re_C}^{\Re_S}\,\{dF_{R,T,A}\} \tag{15}$$

Such as:

$$\begin{bmatrix} dF_X \\ dF_Y \\ dF_Z \end{bmatrix} = \begin{bmatrix} -\sin\eta\,\sin\beta & -\cos\beta & -\cos\eta\,\sin\beta \\ -\sin\eta\,\cos\beta & \sin\beta & -\cos\eta\,\cos\beta \\ \cos\eta & 0 & -\sin\eta \end{bmatrix} \begin{bmatrix} dF_R \\ dF_T \\ dF_A \end{bmatrix}$$

The elementary cutting forces for the totality of N_f teeth [11], [12]:

$$\begin{bmatrix} dF_X(i,j) \\ dF_Y(i,j) \\ dF_Z(i,j) \end{bmatrix} = \sum_{k=1}^{N_f} [T]_{\Re_C}^{\Re_S}(i,j,k) \begin{bmatrix} dF_R(i,j,k) \\ dF_T(i,j,k) \\ dF_A(i,j,k) \end{bmatrix} \tag{16}$$

The elementary cutting forces for the totality can be expressed according to the specific coefficients K_R, K_T and K_A as follows:

$$\begin{bmatrix} dF_X(i,j) \\ dF_Y(i,j) \\ dF_Z(i,j) \end{bmatrix} = \sum_{k=1}^{N_f} [T]_{\Re_C}^{\Re_S}(i,j,k) \begin{bmatrix} K_R \\ K_T \\ K_A \end{bmatrix} f_{z_b}\,\sin[\beta(i,j,k)]\,dz \tag{17}$$

The total cutting force for the j position is:

$$\begin{bmatrix} dF_X(j) \\ dF_Y(j) \\ dF_Z(j) \end{bmatrix} = \sum_{i=1}^{N_Z}\sum_{k=1}^{N_f} [T]_{\Re_C}^{\Re_S}(i,j,k) \begin{bmatrix} K_R \\ K_T \\ K_A \end{bmatrix} f_{z_b}\,\sin[\beta(i,j,k)]\,dz \tag{18}$$

4. SIMULATIONS AND RESULTS

4.1 The case of a flat surface

The model we have presented is applied to the case of a flat surface milling with a ball end tool. The tool used is of a radius R = 10 mm, having two teeth (N_f = 2) and of an helix angle i_0= 10°. This tool fits into the workpiece with a feed of a value f_{zb}= 0.1 mm/tooth, a radial depth A_r= 2 $\cdot R$ = 20 mm and axial depth A_d= 1 mm according to Fig. 6.

Fig. 7 shows the evolution of the cutting forces in the Cartesian coordinate system $\Re_C$. This tool carries out the machining with a tool path along X-axis. In this case, the tool engagement angle in the material, β is located between 0 and π. We note that each of the components is periodic, of a period 2π / N_f. The cutting forces appear since the very beginning of the tool rotation, counted from the Y-axis. They disappear after one angle rotation π where the contact disappears between the first tooth and the material. At this moment the second tooth fits into the matter and we obtain a configuration similar to that of the first period.

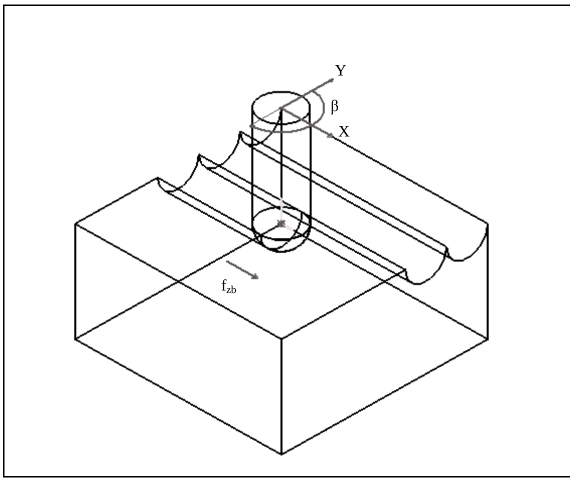

Figure 6: The case of a flat surface milling.

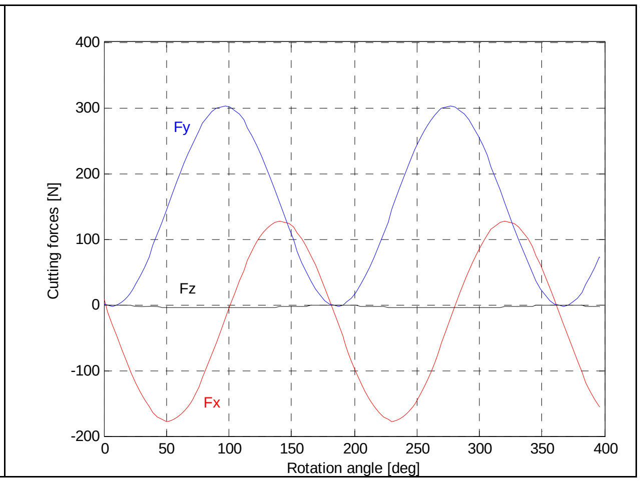

Figure 7: Cutting forces in the case of a flat surface milling.

4.2 Case of an inclined surface

The same model is applied to the case of the milling of an α angle inclined surface, according to the axis-X and of ψ angle according to the axis-Y (see Fig. 8).

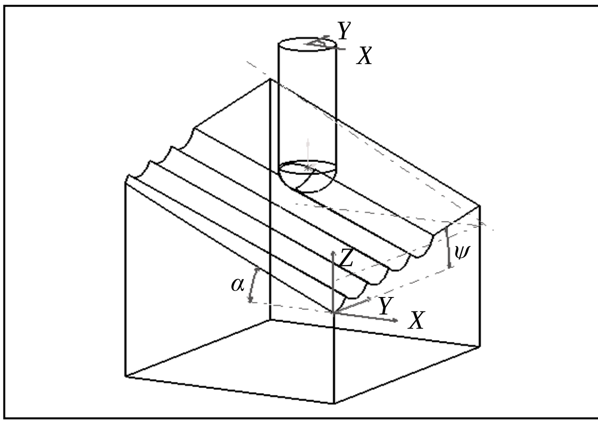

Figure 8: Case of on inclined surface milling.

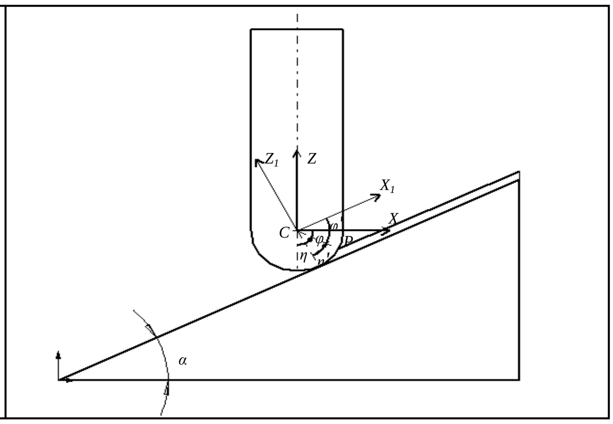

Figure 9: Systems of coordinates in the case of an inclined surface milling.

We designate by $\Re_1$ (C, X_1, Y_1, Z_1) the result of the coordinate system rotation $\Re_0$ (C, X, Y, Z) of an angle α all around the axis-Y. α is the inclination angle of the workpiece surface machining.

The matrix of the passage from $\Re_1$ towards $\Re_0$ denoted $[P]_0^1$ is of the form:

$$[P]_0^1 = \begin{bmatrix} \cos\alpha & 0 & \sin\alpha \\ 0 & 1 & 0 \\ -\sin\alpha & 0 & \cos\alpha \end{bmatrix} \tag{19}$$

The point P is defined in the coordinate system $\Re_1$ by:

$$\overrightarrow{CP} = \begin{pmatrix} R\cos\varphi\sin\beta \\ R\cos\varphi\cos\beta \\ -R\sin\varphi \end{pmatrix} \tag{20}$$

with $\varphi=\pi/2-\eta$.

The point *P* is defined, then, in the coordinate system $\Re_0$, as indicated in Fig. 9:

$$\overrightarrow{CP} = \begin{pmatrix} R\cos\varphi\sin\beta\cos\alpha + R\sin\varphi\sin\alpha \\ R\cos\varphi\cos\beta \\ R\cos\varphi\sin\beta\sin\alpha - R\sin\beta\cos\alpha \end{pmatrix} \tag{21}$$

We designate by $\Re_2$ (C, X_2, Y_2, Z_2), the result of the coordinate system rotation $\Re_0$ (C, X, Y, Z) of an angle ψ around the axis X. ψ is being the second inclination angle of the work-piece machining surface.

The matrix of the passage from $\Re_2$ towards $\Re_1$ denoted $[P]_1^2$ is of the form:

$$[P]_1^2 = \begin{bmatrix} 1 & 0 & 0 \\ 0 & \cos\psi & -\sin\psi \\ 0 & \sin\psi & \cos\psi \end{bmatrix} \tag{22}$$

The matrix of the passage from $\Re_2$ towards $\Re_0$ denoted $[P]_0^2$ is, then, defined by:

$$[P]_0^2 = \begin{bmatrix} \cos\alpha & \sin\alpha\sin\psi & \sin\alpha\cos\psi \\ 0 & \cos\psi & -\sin\psi \\ -\sin\alpha & \cos\alpha\sin\psi & \sin\alpha\cos\psi \end{bmatrix} \tag{23}$$

The point *P* is then defined in the coordinate system $\Re_2$ by :

$$\overrightarrow{CP} = \begin{pmatrix} R\cos\varphi\sin\beta\cos\alpha + R\sin\varphi\sin\alpha \\ R\cos\varphi\sin\beta\sin\alpha\sin\psi + R\cos\varphi\cos\beta\cos\psi - R\sin\varphi\cos\alpha\sin\psi \\ R\cos\varphi\sin\beta\sin\alpha\cos\psi - R\cos\varphi\cos\beta\sin\psi - R\sin\varphi\cos\alpha\cos\psi \end{pmatrix} \tag{24}$$

If we consider the angles *φ'* and *β'* the new reference angles of the active point *P* in the coordinate system $\Re_2$, then, the vector $\overrightarrow{CP}$ coordinates defined in the coordinate system $\Re_2$, verify the following equalities:

$$\begin{cases} R\cos\varphi\sin\beta\cos\alpha + R\sin\varphi\sin\alpha = R\cos\varphi'\sin\beta' \\ R\cos\varphi\sin\beta\sin\alpha\sin\psi + R\cos\varphi\cos\beta\cos\psi - R\sin\varphi\cos\alpha\sin\psi = R\cos\varphi'\cos\beta' \\ R\cos\varphi\sin\beta\sin\alpha\cos\psi - R\cos\varphi\cos\beta\sin\psi - R\sin\varphi\cos\alpha\cos\psi = -R\sin\varphi' \end{cases} \tag{25}$$

Then the angles φ', β' take the following values:

$$\begin{cases} \sin\varphi' = \sin^{-1}(-\cos\varphi\sin\beta\sin\alpha\cos\psi + \cos\varphi\cos\beta\sin\psi + \sin\varphi\cos\alpha\cos\psi) \\ \beta' = \sin^{-1}((\cos\varphi\sin\beta\cos\alpha + \sin\varphi\sin\alpha)/\cos\varphi') \end{cases} \tag{26}$$

with $\varphi' = \pi/2 - \eta'$.

With this change of coordinate system, the milling in the case of an inclined surface can be assimilated to the milling of a plane surface in the coordinate system $\Re_2$. Fig. 10 shows the cutting forces evolution for different values of α and for $\psi=0$.

Fig. 11 presents the evolution of the cutting efforts for different values of ψ and for $\alpha=0$.

4.3 Case of a circular surface

If we consider the milling of a convex or concave circular surface with a curvature radius R_c [5, 6], then, the same principle will be applied to the inclined surface model, with an inclination angle which varies with each increment (Fig. 12).

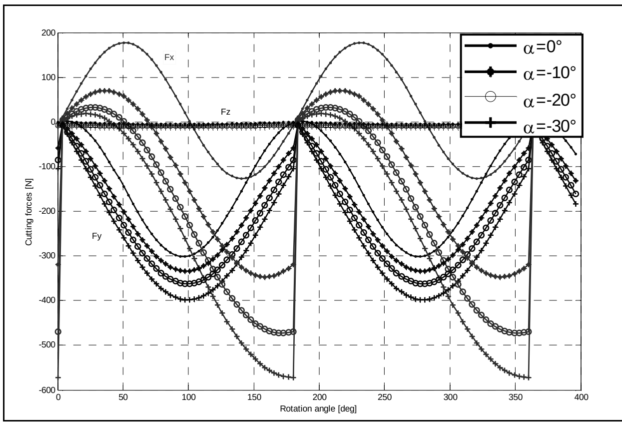

Figure 10: Influence of the inclination angle α upon the evolution of the cutting forces.

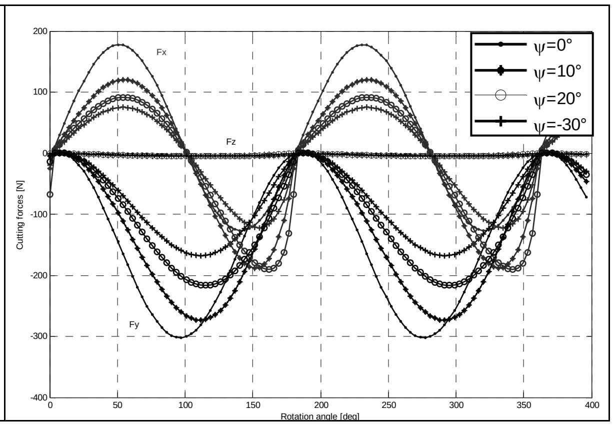

Figure 11: Influence of the inclination angle ψ upon the cutting forces evolution.

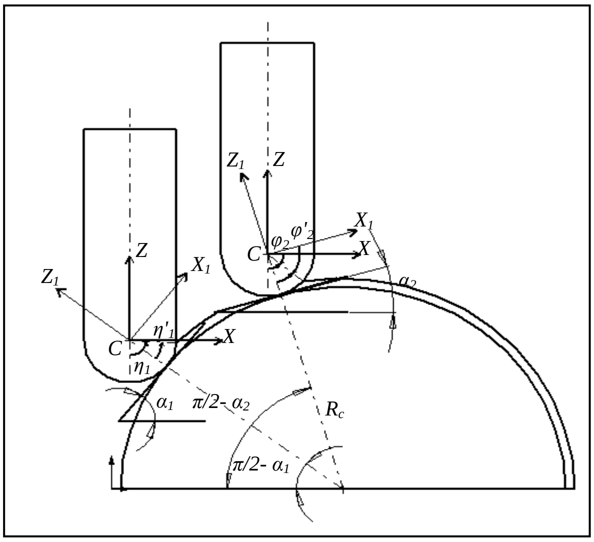

Figure 12: Case of a circular surface milling.

4.4 Application

We would like to carry out the milling of a complex workpiece with a length L= 500 mm and a width l= 100 mm, as indicated in Fig. 13. The surface to be machined comprises a flat part 50 mm in length, a second inclined upward part 100 mm in length and with an inclination angle α_1= 30°, a third part -circular and concave- with a curvature radius R_{c1} = 50 mm, a fourth convex part with a curvature radius R_{c2} = 50 mm, a fifth part, inclined upward, 100 mm in length and with an inclination angle α_1= 30.11° and finally, a sixth part which is flat, 50 mm in length. The tool used here is the same as the one used in the case of a flat surface milling in the same cutting conditions.

Further to the conception of the workpiece to be realised with Mastercam, we could obtain the tool end trajectory. The whole of the coordinates of the points making up this trajectory have been transferred towards Matlab (Fig. 14) so as to make it possible to calculate and draw the corresponding cutting forces.

- ***Longitudinal milling***

The longitudinal milling of the workpiece to be machined is carried out, following the X-axis. Fig. 14 illustrates the tool end trajectory obtained from the coordinates of the points transferred from Mastercam.

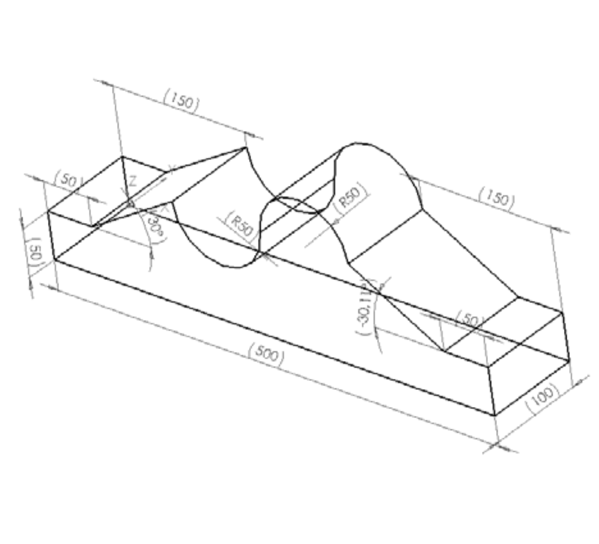

Figure 13: Workpiece conception in 3D.

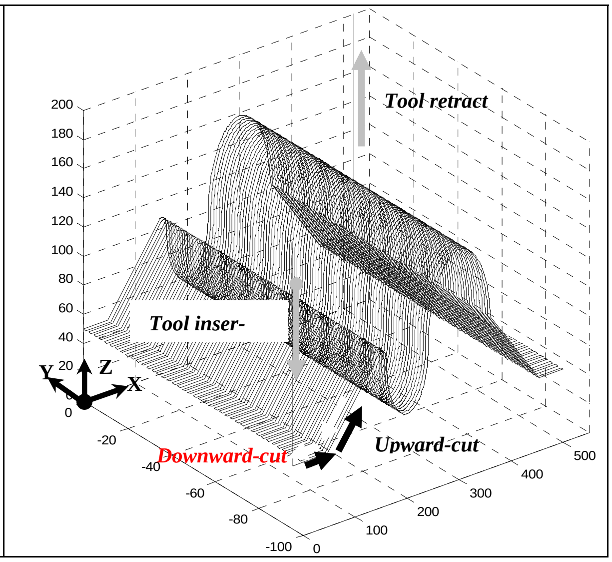

Figure 14: Trajectory of the tool on Matlab.

The cutting forces are calculated according to the nature of the trajectory part to be machined (flat, inclined…) and following the machining direction (following X or –X).

Fig. 15 shows the cutting forces evolution, following the tool end trajectory. This trajectory is of the Zig-Zag type, since the tool carries out several go-and-backs following X and –X, which respectively correspond to an upward cut and a downward cut. The cutting forces are drawn in black for the X machining, and in gray for the –X machining. The F_x and F_y components are represented when multiplied by a coefficient equal to 0.1. This figure shows, also, that the inclination angle α exerts an influence upon the amplitude of the maximum force F_x and F_z, since this amplitude is minimum for an angle tending towards 0, and it increases as α increases in absolute value.

Moreover, the maximum cutting force results F_y and F_z are almost confused for $\alpha = 0°$ in both machining directions: in upward and downward cut, whereas, $|F_{xmax}|$ presents a gap in the case of a flat surface. This gap is justified by the fact that the helix inclined form influences the force sign during the insertion of the tool into the material as shown in Figs. 16 and 17.

Figs. 16 and 17 show a flat surface machining and the corresponding cutting forces in upward and in downward cut. For a fixed coordinate system, the component F_y changes its sign, but keeps the same amplitude. F_z is negative for the two machining signs with the same intensity. However, the component F_x is negative for an upward cut machining, and it presents two parts, one positive and the other negative, at the moment of the downward machining. This positive part influences $|F_{xmax}|$ which decreases for this machining direction.

- ***Transversal milling***

The transversal milling of the part to be machined is carried out following the axis Y.

Fig. 18 represents the tool tip trajectory, obtained from the transferred points coordinates from Mastercam.

Fig. 19 shows the cutting forces evolution, following the tool tip trajectory. This trajectory is of the Zig-Zag type, since the tool carries out several go and backs, following Y and –Y. The cutting forces are drawn in black for the machining following Y, and in gray for the direction –Y. The components F_x and F_y are represented when they are multiplied by a coefficient equal to 0.1. Moreover, this figure shows that the inclination angle α influences the maximum forces amplitude since this amplitude is maximum for an angle tending towards 0, and it decreases as α increases in absolute value.

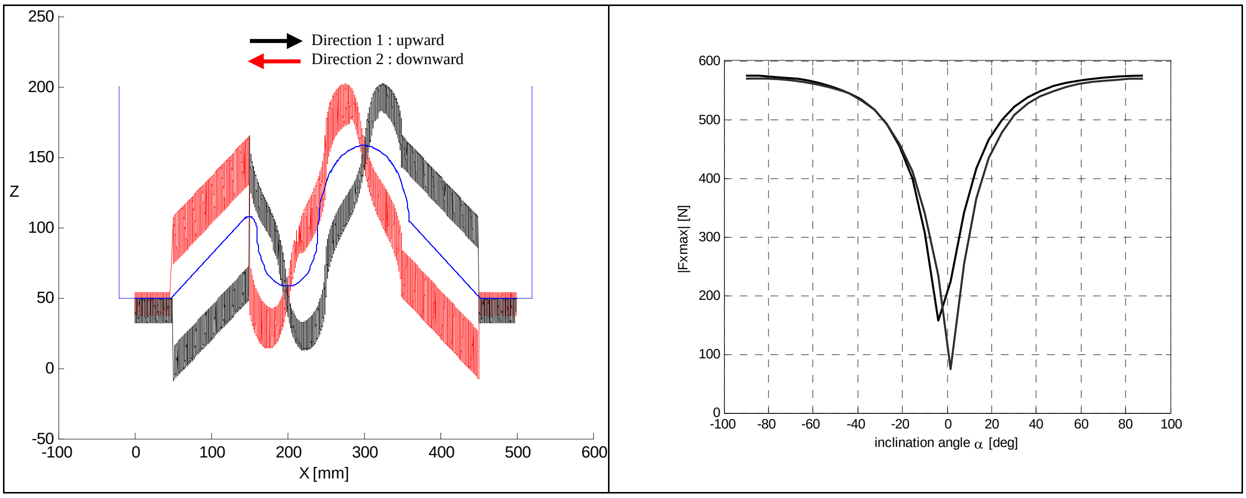

a) $0.1 \times F_x$ d) The effect of the inclination angle α upon $|F_{xmax}|$

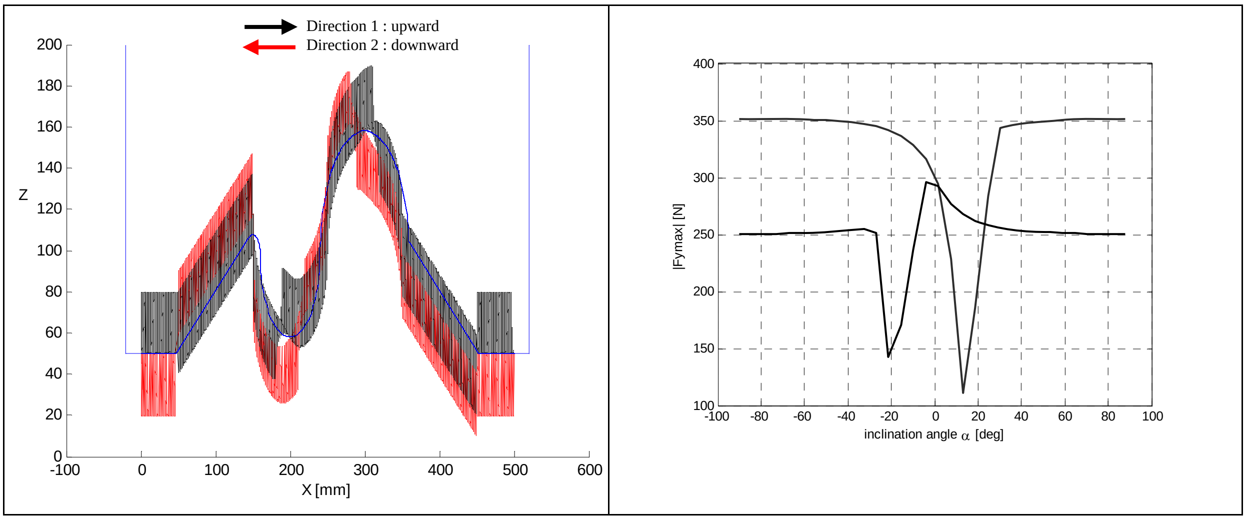

b) $0.1 \times F_y$ e) The effect of the inclination angle α upon $|F_{ymax}|$

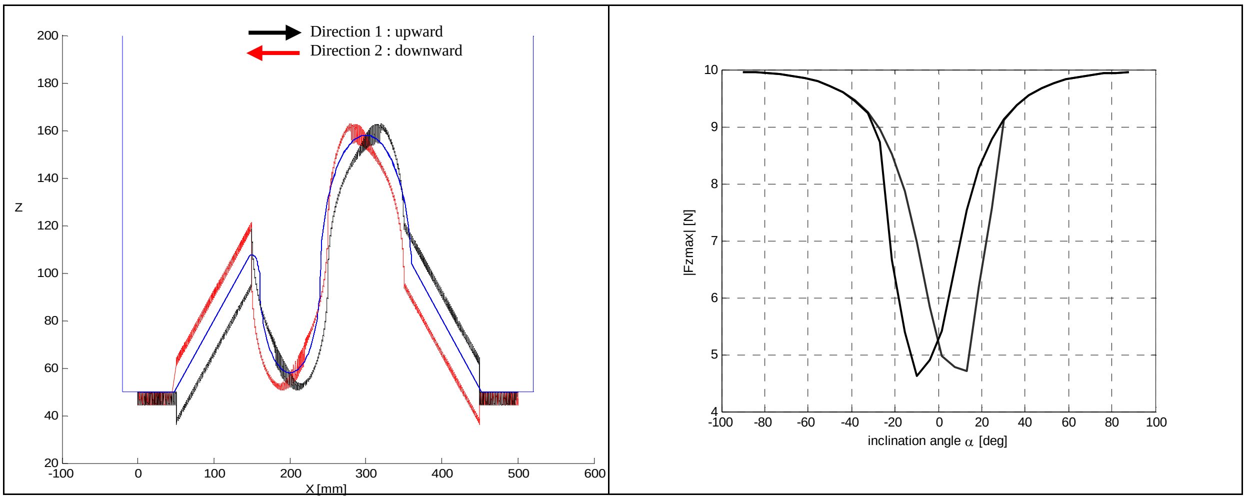

c) F_z f) The effect of the inclination angle α upon $|F_{zmax}|$

Figure 15: Cutting forces simulation in longitudinal milling and the α-inclination angle effect upon the maximum force amplitude.

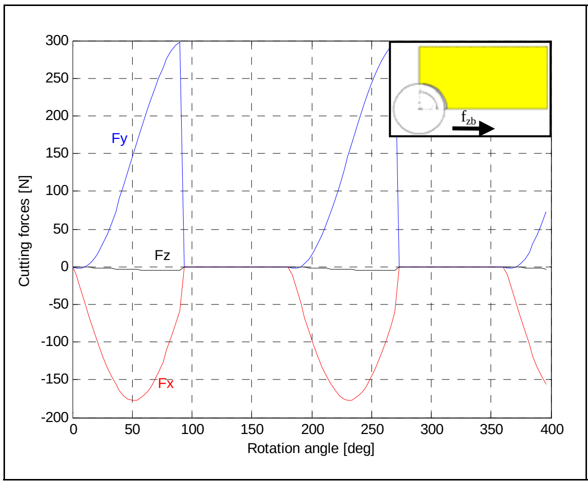

Figure 16: Cutting forces for the case of a flat surface upward-cut milling.

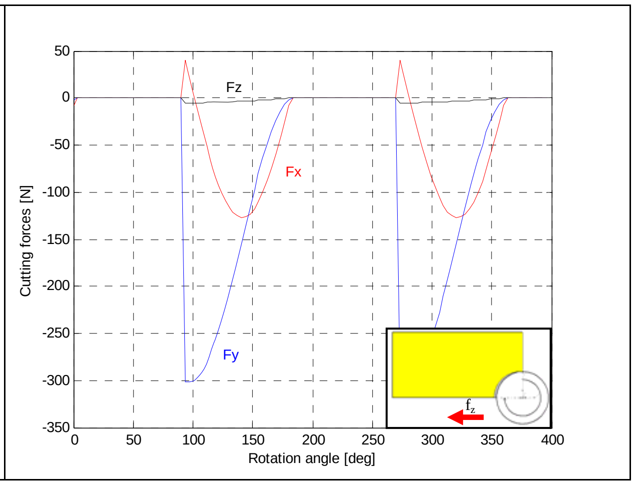

Figure 17: Cutting forces for the case of a flat surface downward-cut milling.

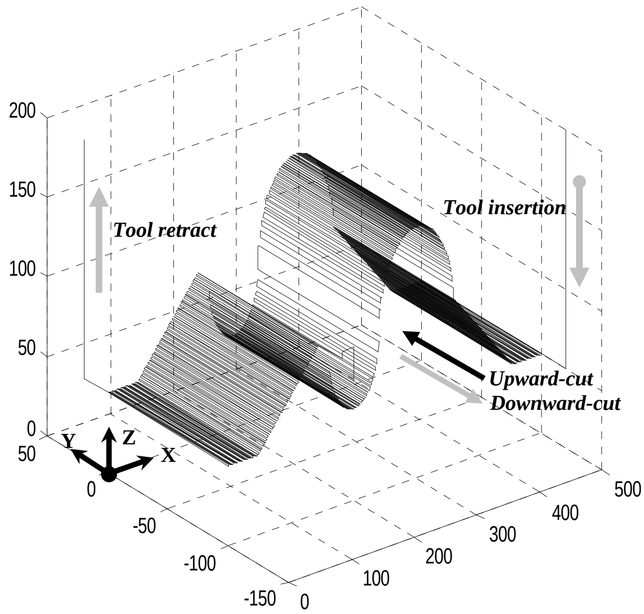

Figure 18: Tool trajectory on Matlab.

Moreover, the maximum cutting force results F_x and F_z are almost confused for $\alpha=0°$ in both directions of the machining (in upward and downward cut), whereas, $|F_{ymax}|$ presents a gap in the case of a flat surface. This gap is justified by the fact that the helix inclined form influences the force sign, during the insertion of the tool into the material.

5. CONCLUSION

In this work, we have proposed a method for modelling and calculating the cutting forces in the case of a hemispherical milling. This method is based on the cutting tool geometrical study.

In fact, the tool spherical part has been discretized in a series of elementary discs, in concordance with the chosen depth of cut. The elementary cutting forces are then calculated. A summation has allowed determining the total cutting force.

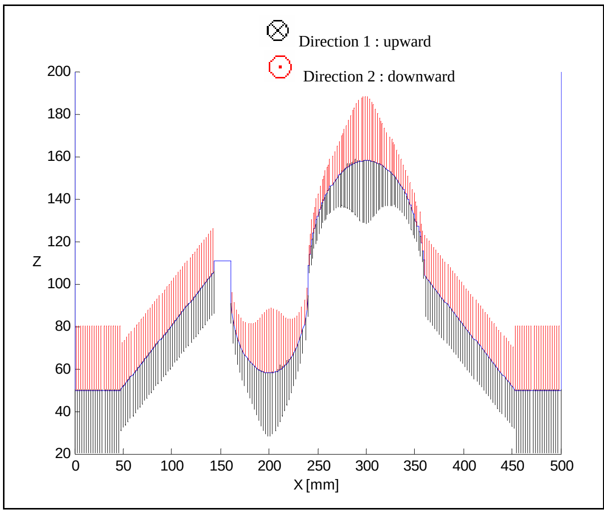

a) $0.1 \times F_x$

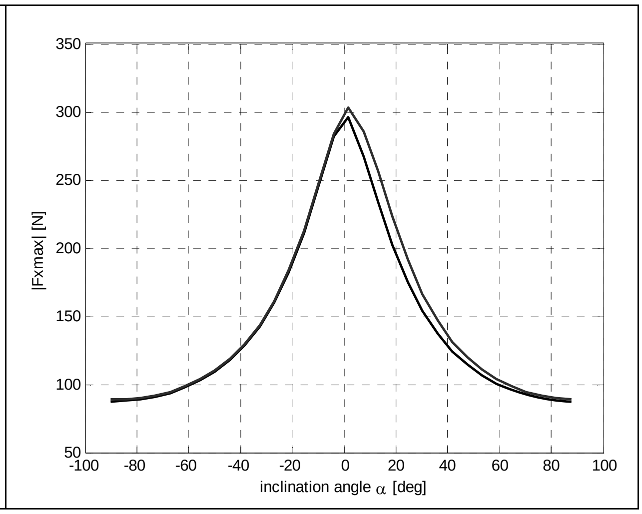

d) The effect of the inclination angle α upon $|F_{xmax}|$

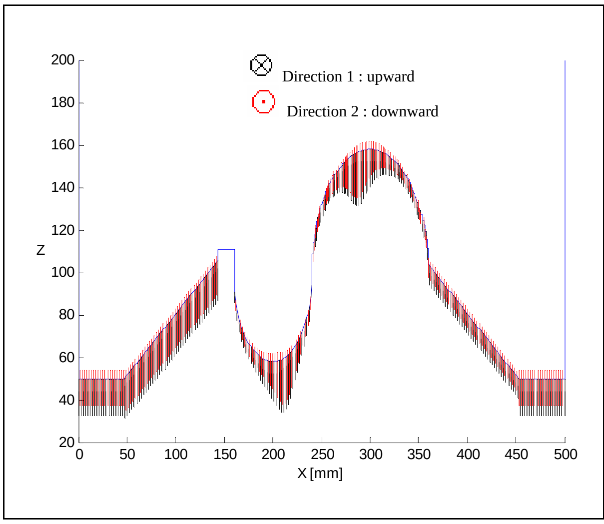

b) $0.1 \times F_y$

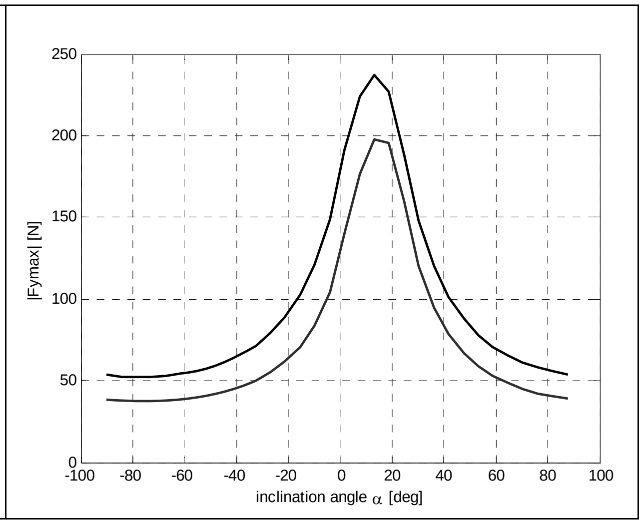

e) The effect of the inclination angle α upon $|F_{ymax}|$

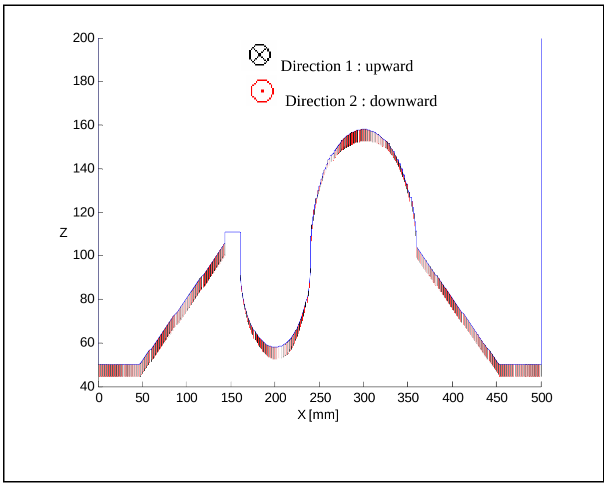

c) F_z

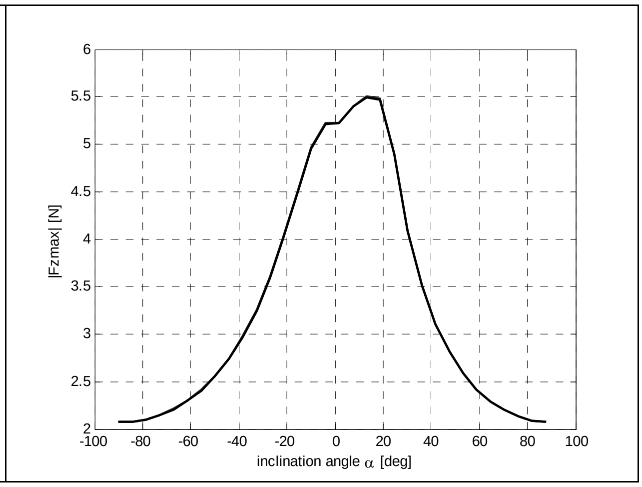

f) The effect of the inclination angle α upon $|F_{zmax}|$

Figure 19: Cutting forces simulation in transversal milling and the α-inclination angle effect upon the maximum force amplitude.

This cutting forces model has been applied in the case of a flat surface. This same model has been used, first of all, in the case of an inclined surface by adopting a reference change which is dependent on the inclination angle. Afterwards, a generalization has been carried out, in the case of a circular surface, by using reference changes according to the inclination angle which varies at each increment all along the trajectory.

For application, we have taken the case of a complex part milling: we have applied the cutting force model, taking into account the nature of the trajectory to be used as well as and the machining sense.

The cutting force model, presented here, is consequently applicable to any type of surface: (plane, inclined, circular). Besides, this model is also valid for a transversal and longitudinal milling. It also takes into consideration the geometrical parameters of the cutting tool used, as well as the machining parameters, such as the axial and radial depth of pass.

Following this study, we consider as perspective to foresee a compensation to correct the trajectory deviation due to the cutting tool deflexion.

REFERENCES

[1] Kim, G. M.; Cho, P. J.; Chu, C. N. (2000). Cutting force prediction of sculptured surface ball-end milling using Z-map, *International Journal of Machine Tools & Manufacture*, Vol. 40, 277–291

[2] Nehez, K.; Csaki, T. (2003). Cutting force modelling possibilities in OPENGL based milling simulators, *Production Systems and Information Engineering*, Miskolc, Vol. 1, 29–39

[3] Fontaine, M.; Moufki, A.; Devillez, A.; Dudzinski, D. (2003). Application de la modélisation thermo-mécanique de la coupe au fraisage boule, *16ème Congrès Français de Mécanique*

[4] Fontaine, M.; Moufki, A.; Devillez, A.; Dudzinski, D. (2007). Modelling of cutting forces in ball-end milling with tool–surface inclination, Part I: Predictive force model and experimental validation, *Journal of Materials Processing Technology*, Vol. 189, 73–84

[5] Fontaine, M.; Moufki, A.; Devillez, A.; Dudzinski, D. (2007). Modelling of cutting forces in ball-end milling with tool–surface inclination, Part II. Influence of cutting conditions, run-out, ploughing and inclination angle, *Journal of Materials Processing Technology*, Vol. 189, 85–96

[6] Yang, M.; Park, H. (1991). The prediction of cutting force in ball end milling, *International Journal of Machine Tools & Manufacture*, Vol. 31, No. 1, 45–54

[7] Lee, P.; Altintas, Y. (1996). Prediction of Ball-End Milling Forces from Orthogonal Cutting Data, *International Journal of Machine Tools and Manufacture*, Vol. 36/9, 1059-1072

[8] Boujelbene, M.; Moisan, A.; Tounsi, N.; Brenier, B. (2004). Productivity enhancement in dies and molds manufacturing by the use of C1 continuous tool path, *International Journal of Machine Tools & Manufacture*, Vol. 44, 101–107

[9] Martellotti, M. E. (1941). An Analysis of the Milling Process, *Transactions of ASME*, Vol. 63, 667

[10] Milfelner, M.; Cus, F. (2003). Simulation of cutting forces in ball-end milling, *Robotics and Computer Integrated Manufacturing*, Vol. 19, 99–106

[11] Ikua, B. W.; Tanaka, H.; Obata, F.; Sakamoto, S. (2001). Prediction of cutting forces and machining error in ball end milling of curved surfaces -I theoretical analysis, *Precision Engineering Journal of the International Societies for Precision Engineering and Nanotechnology*, Vol. 25, 266–273

[12] Ikua, B. W.; Tanaka, H.; Obata, F.; Sakamoto, S.; Kishi, T.; Ishii, T. (2002). Prediction of cutting forces and machining error in ball end milling of curved surfaces –II Experimental verification, *Precision Engineering Journal of the International Societies for Precision Engineering and Nanotechnology*, Vol. 26, 69–82